

## Characterization of fluid flow in a microchannel with a flow-disturbing step

Ioannis A. STOGIANNIS<sup>1</sup>, Agathoklis D. PASSOS<sup>1</sup>, Aikaterini A. MOUZA<sup>1</sup>, Spiros V. PARAS<sup>1\*</sup>,  
Vera PENKAVOVA<sup>2</sup>, Jaroslav TIHON<sup>2</sup>

\* Corresponding author: Tel.: ++30 2310 996174; Email: [paras@auth.gr](mailto:paras@auth.gr)

<sup>1</sup> Chemical Engineering Department, Aristotle University of Thessaloniki, GR

<sup>2</sup> Institute of Chemical Process Fundamentals, Academy of Sciences of the Czech Republic, CZ

**Abstract** The flow around a flow-disturbing step in a rectangular microchannel is studied by measuring the wall shear rate along the channel, using the *electrodiffusion technique* and by determining the velocity field using the  $\mu$ -PIV method. A parametric study based on the *Design of Experiments (DOE)* and the *Response Surface Methodology (RSM)* was then performed, and the effect of key design parameters on the flow characteristics was numerically investigated using *CFD* simulations. The computational results are in excellent agreement with the corresponding experimental ones. The *CFD* simulations cover both the laminar and the turbulent flow regime. It was revealed that in both flow regimes the step height has a major influence on the recirculation length. However, the Reynolds number ( $Re$ ) value affects the recirculation length only in the laminar region, while the step length seems to have no significant effect compared to the  $Re$  and the step height. Finally, new correlations are proposed predicting the length of the bottom recirculation zone with reasonable accuracy and can be used as rough guidelines for the design of microdevices.

**Keywords:** Microchannels, wall shear stress, micro-PIV, *CFD*

### 1. Introduction

The intensive development of Microfluidic technologies resulted in a considerable range of microfluidic systems for a variety of applications. The results of this research and the technology explosion in the last decade has led to the identification of Microfluidics as one of the most promising fields in modern process engineering. The main advantages of micro-systems are their high surface-to-volume ratio, the increased efficiency and operability of the micro-devices and the enhancement of fluid mixing, a fundamental unit operation for many other processes (Kockmann, 2006).

In the microscale, mixing can be induced both by active and passive methods. In passive micromixers, there is no need for external energy, while the mixing performance is enhanced by modifying the flow path, creating and increasing contact time between fluids. In the macroscale, the flow over a *Backward Facing Step (BFS)* is considered a benchmark and has been thoroughly studied either experimentally (e.g. Armaly et al., 1983) or numerically

(e.g., Le et al., 1997). The study of liquid flow in a *BFS* geometry in a microchannel has recently attracted interest. Kherbeet et al. (2014) studied a *BFS* geometry in a microchannel and reported that the basic features observed in in the macroscale (like velocity profiles and recirculation areas) remain practically the same in the microscale.

In heat transfer applications a typical modification of the channel wall is an orthogonal barrier, effectively creating a step in the fluid flow path that significantly enhances heat transfer by modifying the flow field (Stogiannis et al., 2013). Although the flow in simplified standard geometries like backward or forward facing steps has been extensively studied, to the authors' best knowledge limited research have been done for the flow-disturbing steps.

The experimental characterization of fluid flow in microscale presupposes the use of a reliable measuring technique, but the well-established methods in macroscale are not easily applicable in microchannels. Due to the small dimensions of the conduits it is challenging to

employ methods that use flush-mounted sensors like the *electrodiffusion technique* (Hanratty and Campbell, 1996) typically used for near-wall flow diagnostics in larger scales. Thus non-intrusive techniques like *micro-Particle Image Velocimetry* ( $\mu$ -PIV) have been extensively used in microfluidics for two-dimensional velocity-field measurements (Koutsiaris et al., 1999) and the investigation of liquid film characteristics (Anastasiou et al., 2013).

It is common practice in fluid flow studies to replace expensive and time-consuming experiments with, previously validated, *Computational Fluid Dynamics* (CFD) simulations. The CFD codes are used in order to assess the effect of important geometrical characteristics of the microchannels on various design parameters like the extent of recirculation zones in passive micromixers (Mouza et al., 2005).

The scope of this work is to characterize the flow around a flow-disturbing step aiming to investigate the effect of key design parameters on the size of the *reattachment length* of the recirculation zones. These parameters have been identified as the most important in applications of microchannels like fluid mixing and heat transfer enhancement. In the macroscale it has been found that the reattachment length depend primarily on the geometrical characteristics of the channel and the fluid  $Re$  (Tihon et al., 2001). A CFD code is validated using experimental data from two independent methods, namely  $\mu$ -PIV for investigating the velocity field and the electrodiffusion technique for local measurement of the *Wall Shear Stress* (WSS). Finally, using the validated CFD code a parametric study is performed based on *Design of Experiments* (DOE) and *Response Surface Methodology* (RSM) techniques.

## 2. Experimental Setup

We conducted experiments in a rectangular PMMA channel (0.925mm in height, 10mm in width and 100mm in length) with a step (0.400mm in height) located at a distance of 6cm from the inlet (**Fig. 1**). The channel geometry is completed by placing the top wall. The use of an O-ring prevents leakage. The ratio of the channel width over the step height gives the spanwise aspect ratio ( $AR$ ) which is a critical

parameter for the distinction between 2D and 3D flow. Tihon et al. (2010) showed that separating/reattaching flow is always affected by the value of  $AR$ , but for  $AR$  greater than 25 it can be characterized as predominantly 2D.

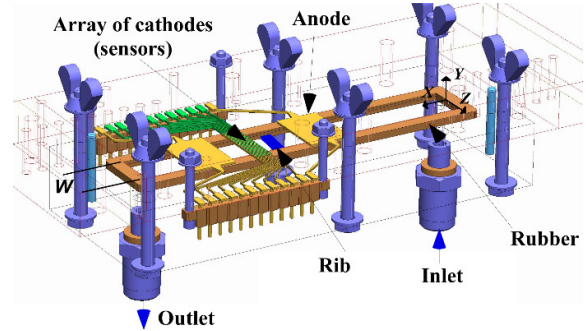


**Fig. 1.** 3D reconstruction of the microchannel with electrodiffusion microsensors.

The *electrodiffusion technique*, which is based on the measurement of the limiting diffusion current of the ferricyanide ions reduction at a small working electrode, is used to measure local values of wall shear rate (Hanratty and Campbell, 1996). For a single strip segment the current-signal,  $I$ , can be related to the instantaneous value of wall shear rate,  $s_w$ , through the formula:

$$I = 0.807 z F c_0 w l^{2/3} D^{2/3} s_w^{2/3}$$

where  $z$  is the number of electrons involved in the electrochemical reaction,  $F$  is the Faraday constant,  $l$  is the length of the strip in the main flow direction,  $w$  is its width, while  $c_0$  is the bulk concentration of the ions and  $D$  their diffusivity in the solution. The working solution is water containing 0.025M  $K_3[Fe(CN)_6]$ , 0.025M  $K_4[Fe(CN)_6]$  and 0.057M  $K_2SO_4$  as a supporting electrolyte.

The micro sensors consist of twenty micro-cathodes of 160 $\mu$ m length each, placed at a distance of 40 $\mu$ m from each other and flush-mounted on the top wall of the microchannel (above the step). A larger anode is positioned away from the step inside the channel. The  $\mu$ -structures were built on the channel wall using a *UV-lithography* technique while they are later filled with gold using galvanic deposition as described in detail elsewhere (Schrott et al., 2009). The wall shear-rate profile at various positions before and after the step can be measured by shifting the top wall of the microdevice

along the  $X$ -axis. The test fluid is supplied from a constant temperature tank (25°C) using a gear pump.

The  $\mu$ -PIV is an optical non-intrusive technique intended for measuring two-dimensional velocity fields. The method is based on tracing fluorescent particles that are seeded in the working fluid. These particles should be small enough to accurately follow the fluid motion and avoid microchannel obstruction and at the same time large enough to be successfully imaged and to avoid Brownian motion. The local velocity can be estimated by the displacement of a group of particles over a known time interval between two successive images.

The experimental setup consists of a fluorescence  $\mu$ -PIV system (Anastasiou et al., 2013), the experimental microchannel, a gear pump and a bath for maintaining constant fluid temperature. The measuring section of the microchannel was illuminated by double cavity  $Nd:YAG$  laser emitting at 532nm. The flow was recorded by a high sensitivity  $CCD$  camera (*Hisense MkII*), connected to a Nikon (*Eclipse LV150*) microscope which moves along the vertical axis ( $Y$ -axis in **Fig. 1**) with accuracy of one micron. The flow was traced by adding Nile fluorescent microspheres with a mean diameter of 1 $\mu$ m. A 20x air immersion objective with  $NA=0.20$  was used, which results to 3 $\mu$ m depth of field. The time delay between frames is in the range of 50-1000 $\mu$ s, depending on the flow rate, while the sampling rate is 11Hz.

Velocity measurements were performed at specific planes along the vertical axis (50 $\mu$ m distance from each other) at 1mm before and 0-2mm after the step. In order to estimate the velocity field 50 images were acquired in every plane. Image processing and velocity calculation was performed using the *Flow Manager* software (*Dantec Dynamics*).

### 3. Numerical Calculations

The velocity field is visualized using a  $CFD$  code (i.e. *ANSYS CFX*<sup>®</sup> 15.0) while the computational geometry and mesh is designed using the parametric features of *ANSYS Workbench*<sup>®</sup> package. The microchannel is modeled as a 3D computational domain since it has been proved that in similar *BFS* geometries the flow can be

three-dimensional in nominally two-dimensional geometries (Kaiktsis et al., 1991). A uniform pure hexahedral mesh is used to discretize the computational space. The size of the grid is  $\sim 4 \times 10^6$  cells resulting in a spatial resolution after the step of 30 $\mu$ m and 10 $\mu$ m for the  $X$ - and  $Y$ -axis respectively. To reduce the computational cost, a vertical symmetry plane is placed along the flow direction.

Initially, we designed a computational geometry identical to the microchannel used in the experimental study, i.e. including the inlet and outlet of the fluid perpendicular to the flow direction. Using preliminary  $CFD$  simulations it has been proved that for the geometrical characteristics imposed by the specific microdevice the flow is fully developed before reaching the step for all the  $Re$  values used in this study. As a result, it is possible to ignore the inlet and the outlet effects and to impose a fully developed boundary condition for the inlet before the step; no-slip condition is employed on channel walls, while a constant atmospheric pressure is applied on the outlet. The *Direct Numerical Simulation (DNS)* scheme is used for the laminar flow regime whereas the two-equation  $k-\omega$  turbulence model is used for the rest of the  $Re$  range.

We introduced three dimensionless groups (**Fig. 2** and **Table 1**) as design variables for the  $CFD$  simulations, namely:

- the step aspect ratio ( $l/d$ ), defined as the length of the step ( $l$ ) divided by its height ( $d$ ),
- the ratio of step height to channel height ( $d/H$ ), i.e., the magnitude of the channel blockage,
- the  $Re$ , using as characteristic length the channel height ( $H$ ).

The spanwise channel aspect ratio was kept constant and identical to the experimental device.

Depending on the  $Re$  value the appropriate numerical model (i.e. laminar or turbulent model) is applied for solving the *Navier-Stokes* equations. A summary of the design variable ranges are given in **Table 1**. Employing the *Design Exploration* features of *ANSYS Workbench*<sup>®</sup> package a set of “*computational experiments*” has been designed based on the well-

established *Box-Behnken DOE* method. The recirculation length can be expressed as a function of the design variables (**Fig. 2**), using the *Response Surface Methodology (RSM)*.

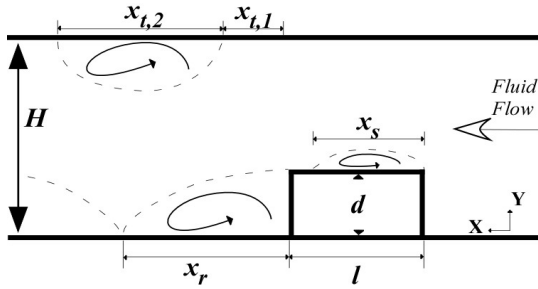


**Fig. 2.** Geometrical parameters of the microchannel and recirculation lengths.

**Table 1** Constraints of the design variables.

Parameter	Lower bound	Upper bound
$d/H$	0.4	0.8
$l/d$	2	16
$Re$ (laminar)	100	360
$Re$ (turbulent)	650	1600

#### 4. CFD Validation

The *CFD* code used for performing the parametric study is validated using experimental data acquired by two methods, i.e. the  $\mu$ -*PIV* and the *electrodiffusion technique*.

The  $\mu$ -*PIV* is used to measure 2D velocity fields using the appropriate objectives. The velocity profile along the *Y*-axis (**Fig. 3**- red line) is reconstructed by consecutive velocity fields (on *XZ* planes) acquired by varying the focusing distance of the microscope. The numerical results for both the laminar (**Fig. 3a**) and the turbulent (**Fig. 3b**) region are in excellent agreement with the  $\mu$ -*PIV* measurements. It should be noted that a recirculation zone is predicted for both  $Re$ .

We have verified the reliability of the numerical simulation at the close to wall region by comparing the *CFD* results with data obtained by the *electrodiffusion technique*. The performance of the *CFD* code in these regions is critical, as unsuitable design of the grid can lead to unreliable results. The *electrodiffusion* sensors are placed on the roof of the microchannel (**Fig. 4** – red line).

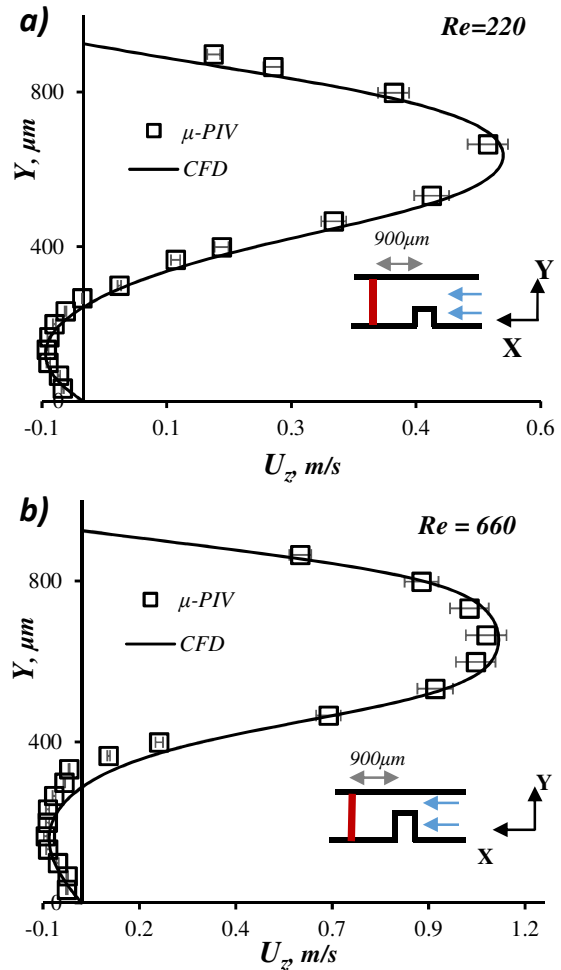


**Fig. 3.** Velocity profile reconstruction from  $\mu$ -*PIV* data and comparison with *CFD* simulation for the a) laminar, b) turbulent region.

There is an excellent agreement between the shear rate measured by the *electrodiffusion technique* and the shear rate calculated by the *CFD* code. The shear rate values are always positive along the channel length, which implies that there is no recirculation zone on the wall above the step for this  $Re$ . Using the *CFD* code for the same geometrical characteristics of the experimental microchannel, we can investigate the effect of the flow rate on the extent of the bottom recirculation zone, i.e.  $x_r$  (**Fig. 2**), a parameter that has been extensively studied in *BFS* geometries in the macroscale. The  $x_r$  value is calculated at the channel centerline, i.e. away from the sidewalls. This can be considered the maximum  $x_r$  for each  $Re$  as the effect of the walls leads to smaller recirculation zones on the two sides of the channel (Tylli et al., 2002).

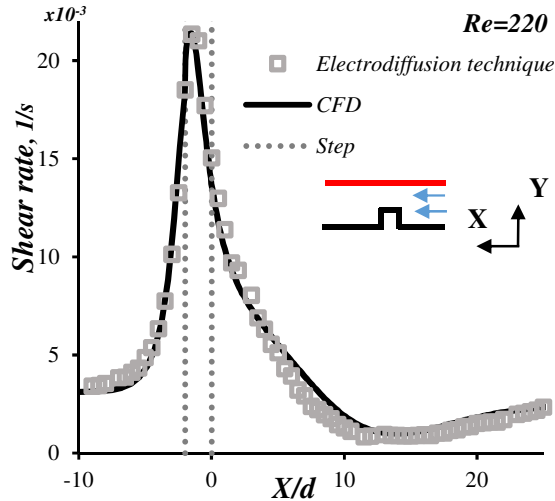


Fig. 4. Shear rate on the wall above the step using the electrodiffusion technique and comparison with CFD.

In Fig. 5 the  $x_r/d$  value is shown for the range of  $Re$  used in this study. It can be seen that up to  $Re \approx 600$ , i.e. in the laminar region  $x_r$  increases linearly with  $Re$ . For  $Re > 600$ , i.e. in the turbulent region,  $x_r/d$  decreases and quickly reaches a constant value (at  $x_r/d \approx 13.5$ ) up to the maximum  $Re$  studied.

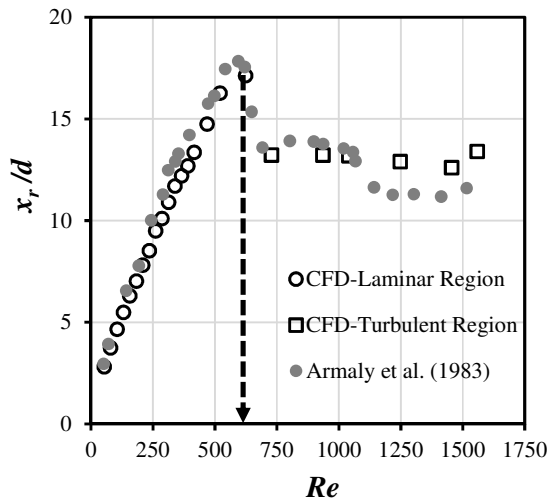


Fig. 5. Dependence of bottom reattachment length  $x_r$  with the  $Re$  and comparison with BFS data.

Results are compared with experimental data from the pioneer study by Armaly et al. (1983) where a macroscale *BFS* geometry was used and was designed for 2D flow and  $d/H=0.5$ . These design parameters are similar with the microdevice used in this approach. The  $Re$  used by Armaly et al. (1983) is properly transformed in order to meet the definitions of this study.

From Fig. 5 we can clearly observe that Armaly’s experimental data are in very good agreement with CFD results. We can deduce that for the same geometrical characteristics of the channel the effect of  $Re$  on  $x_r$  is practically the same in a *BFS* and a step geometry.

## 5. Recirculation zones

The numerical simulations were initially divided in two major groups depending on the type of flow prevailing inside the microchannel (laminar/turbulent region). The existence of recirculation zones (Fig. 2) is investigated for all the “computational experiments” resulted from the *DOE* methodology. The influence of the three dimensionless parameters (i.e.  $Re$ ,  $l/d$  and  $d/H$ ) on the formation of recirculation zones inside the microchannel was investigated by the CFD simulations.

In the laminar region, the  $Re$  ranges from 100 to 360 while the values of  $d/H$  correspond to channel blockages of 40%, 60% and 80% respectively (Table 1). The upper bound of  $Re$  is properly selected so as to be possible to use a laminar model for all channel blockages. The step length varies from  $l/d=2$  (i.e., a relatively steep step) to  $l/d=16$ , a value, which is eventually possible to compare with the *BFS* case. The results indicate that the length of the recirculation zone  $x_r$  is strongly affected by the  $Re$  and the blockage of the channel while the length of the step seems to have less effect on  $x_r$ . More specifically, when the blockage ratio increases from 40% to 80% (i.e. doubling the step height), while the remaining design parameters are kept constant, the bottom recirculation length is increased by 70% (Fig. 6). In addition,  $x_r$  is almost doubled when the flow rate and consequently  $Re$  increases from 100 to 360. This result is in agreement with the previous observation in the laminar region where  $x_r$  depends almost linearly on  $Re$  (Fig. 5).

A recirculation zone located on top of the step ( $x_s$  in Fig. 2), typical in *Forward Facing Steps* (Sherry et al., 2010), has been also observed for 60% blockage values and high  $Re$ . In all cases,  $x_s$  is significantly shorter than the length of the step. In the laminar region, the recirculation zones located at the upper wall of the channel ( $x_{r,1}$  and  $x_{r,2}$  in Fig. 2) has been also

observed in the majority of the simulations, with the total length ranging from  $(x_{i,2}/d)=9$  up to  $(x_{i,2}/d)=18$ . The formation of this type of recirculation zone is also mainly affected by the channel blockage and the flow rate whilst it is not affected by the length of the step.

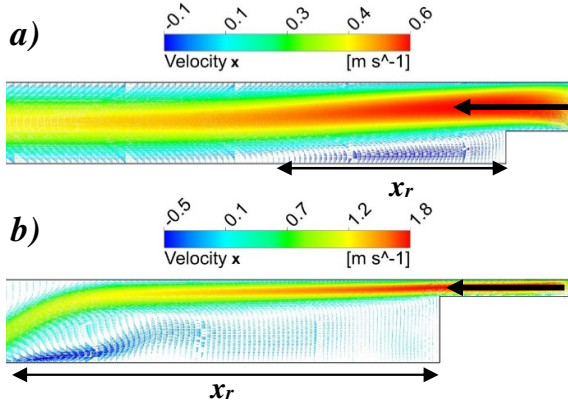


**Fig. 6.** Recirculation zone at the bottom of the channel for  $Re=230$  and  $l/d=2$ : a)  $d/H=0.4$  and b)  $d/H=0.8$ .

In the turbulent region, the  $Re$  ranges from 650 to 1600, while both the channel blockage and the step length are kept unchanged. The blockage ratio has practically the same effect on the formation of the bottom recirculation zone as it has in the laminar region. For example, the recirculation length  $x_r$  increases by 60% when the blockage ratio increases from 40% to 80% (**Fig. 7**)

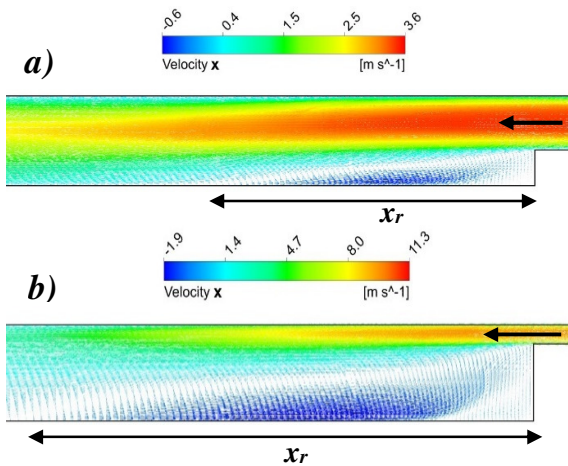


**Fig. 7.** Recirculation zone at the bottom of the channel for  $Re=1600$  and  $l/d=9$ : a)  $d/H=0.4$  and b)  $d/H=0.8$ .

On the contrary, the flow rate in the turbulent region seems to have no significant effect on  $x_r$ , which agrees with the behavior observed previously in **Fig. 5**. For  $d/H$  values greater than 0.6 a secondary recirculation zone,  $x_c$ , is

observed at the corner of the step whereas there are no recirculation regions at the top wall of the channel. As for the parameter corresponding to the step length  $l/d$ , its effect on the recirculation zones formation is insignificant, a fact that is in accordance with the results of the laminar region.

## 6. Parametric study

In channels employed with wall modifications it has been proved (Nie and Armaly, 2004) that the enhancement of heat transfer and fluid mixing is mainly affected by the bottom recirculation zone (characterized by  $x_r$  length). The aim of this parametric study is to quantify the effect of geometrical characteristics of the channel (expressed as dimensionless design variables) on the bottom recirculation length based on the “computational experiments”. The DOE methods allow the designer to extract as much information as possible from a limited number of test cases and makes the method ideal for CFD models that can be significantly time-consuming (Stogiannis et al., 2013).

Using the RSM two second-order polynomial equations (one for the turbulent and one for the laminar region) are developed and expressed as:

$$x_r/H = a_0 + \sum_{j=1}^k a_j x_j + \sum_{j=1}^k a_{jj} x_j^2 + \sum_{i \neq j}^k \sum_{i \neq j}^k a_{ij} x_i x_j$$

where  $\alpha_{ij}$  are the unknown coefficients of the polynomial equation (**Table 2**) determined using the calculated values of  $x_r/H$  for the prescribed set of design points. In similar studies where the effect of step height was assessed the non-dimensional quantity  $x_r/H$  was used in order to be independent of the design variable  $d/H$  (Chen et al., 2006).

The correlations produced by the RSM can be used to check the effect of a certain design variable on the  $x_r$  while keeping the other parameters constant. In **Fig. 8a** the recirculation length for the laminar region is calculated as a function of  $d/H$  for three values of  $Re$ , namely the lower bound, the upper bound and the middle value of the range studied. It is clear that the same pattern is followed for all  $Re$ , where recirculation length increases by increasing the step height up to a value of  $d/H=0.65$  where it

reaches a peak and then it decreases up to  $d/H=0.8$  which is the limit in this study.

**Table 2** Values of the coefficients of the quadratic models for laminar and turbulent regions.

Laminar	$I$	$d/H$	$l/d$	$Re$
$I$	-14.10			
$d/H$	44.42	-31.97		
$l/d$	0.12	-0.03	5.01E-3	
$Re$	0.03	3.33E-3	-8.53E-5	-2.95E-5

Turbulent	$I$	$d/H$	$l/d$	$Re$
$I$	2.43			
$d/H$	4.37	1.59		
$l/d$	0.12	0.08	1.10E-4	
$Re$	6.03E-4	-7.95E-4	-1.06E-4	1.86E-7

On the other hand, in the turbulent region the recirculation length  $x_r$  increases linearly with  $d/H$ , if the remaining design variables are kept constant (**Fig. 8b**). As it was expected (**Fig. 5**), the effect of  $Re$  is more pronounced in the laminar region. From **Fig. 8b** we also reveal that the difference between the three  $Re$  numbers is less than 10%.

The effect of the  $l/d$  design variable on  $x_r$  recirculation length is significantly smaller than that of the other two design variables. The polynomials produced by the *RSM* can provide a rough guideline for the initial design of micro-devices employed with flow disturbing steps.

## 7. Conclusions

We studied the flow around a flow-disturbing step located inside a rectangular microchannel both numerically and experimentally. Experimental data of velocity (acquired by a  $\mu$ -PIV system) and wall shear stresses using appropriate microsensors integrated into the wall of the microdevice were used to validate a *CFD* code, then applied for the continuation of the study. It was found that the numerical results were in excellent agreement with the experimental ones.

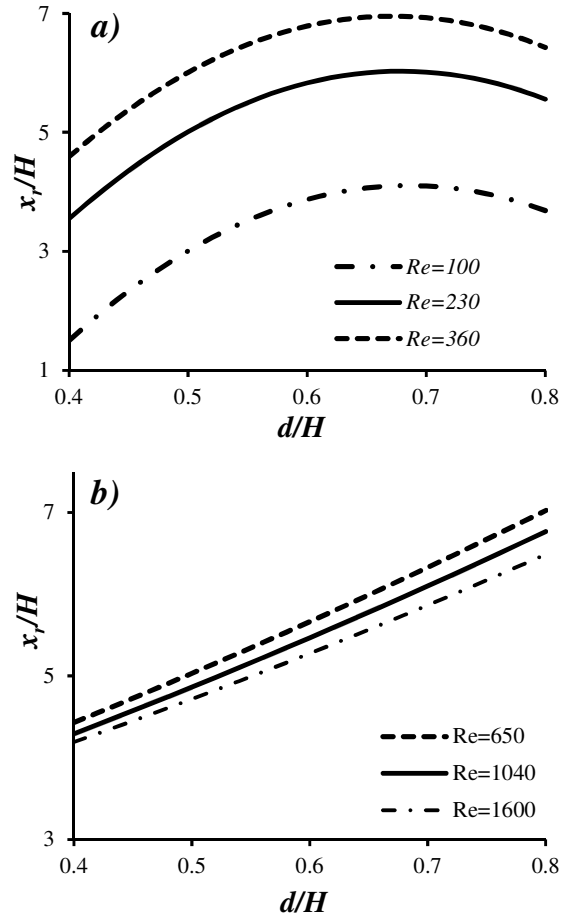


**Fig. 8.** Effect of step height ( $d/H$ ) on the recirculation length for three  $Re$  numbers a) laminar region, b) turbulent region.

The key outcomes of this work are as follows:

- The results of this study follow practically the same trend as the experimental data from previous studies concerning the bottom recirculation length after a *BFS*.
- The validated *CFD* code was used for identifying the recirculation zones around the step. It has been revealed that the extent of the recirculation zones are mainly affected by  $d/H$  ratio and the  $Re$  number.
- It was found that, in the laminar region, the bottom reattachment length increases with  $d/H$  only up to a critical value, while in the turbulent region it increases linearly with  $d/H$  for the whole range studied.
- Based on the parametric study we have formulated design correlations that can predict the length of the principal recirculation zone. The proposed design equations can be used

as rough guidelines for the design of mixers and heat exchangers in the microscale.

More work is certainly needed (e.g. experimental data for different geometrical characteristics of the channel) and is currently in progress to check the validity of the proposed correlations.

**Acknowledgements:** Authors would like to thank the Lab technician Mr. A. Lekkas for the construction and installation of the experimental apparatus and Dr. A.D. Anastasiou for his help with the  $\mu$ -PIV. The financial support from the “Greece – Czech Republic Bilateral Projects 2011-2013” (EIIAN II-EII-11CZ\_18\_ET29) is gratefully acknowledged.

## 8. References

- Anastasiou, A.D., Makatsoris, C., Gavriilidis, A., Mouza, A.A., 2013. Application of  $\mu$ -PIV for investigating liquid film characteristics in an open inclined microchannel. *Exp. Therm. Fluid. Sci.* 44, 90-99.
- Armaly, B.F., Durst, F., Pereira, J.C.F., Schonung, B., 1983. Experimental and Theoretical Investigation of Backward-Facing Step Flow. *J. Fluid Mech.* 127, 473-496.
- Chen, Y.T., Nie, J.H., Armaly, B.F., Hsieh, H.T., 2006. Turbulent separated convection flow adjacent to backward-facing step-effects of step height. *Int. J. Heat Mass Tran.* 49, 3670-3680.
- Hanratty, T.J., Campbell, J.A., 1996. Measurement of wall shear stress, in: Goldstein, J. (Ed.), *Fluid mechanics measurements*. Taylor & Francis, Washington, DC, pp. 575-648.
- Kaiktsis, L., Karniadakis, G.E., Orszag, S.A., 1991. Onset of three-dimensionality, equilibria, and early transition in flow over a backward-facing step. *J. Fluid Mech.* 231, 501-528.
- Kherbeet, A.S., Mohammed, H.A., Munisamy, K.M., Salman, B.H., 2014. The effect of step height of microscale backward-facing step on mixed convection nanofluid flow and heat transfer characteristics. *Int. J. Heat Mass Tran.* 68, 554-566.
- Kockmann, N., 2006. *Micro process engineering: fundamentals, devices, fabrication, and applications*. Wiley-VCH, Weinheim.
- Koutsiaris, A.G., Mathioulakis, D.S., Tsangaris, S., 1999. Microscope PIV for velocity-field measurement of particle suspensions flowing inside glass capillaries. *Meas. Sci. Technol.* 10, 1037-1046.
- Le, H., Moin, P., Kim, J., 1997. Direct numerical simulation of turbulent flow over a backward-facing step. *J. Fluid Mech.* 330, 349-374.
- Mouza, A.A., Pantzali, M.N., Paras, S.V., Tihon, J., 2005. Experimental and numerical study of backward-facing step flow, 5th National Chemical Engineering Conference, Thessaloniki, Greece.
- Nie, J.H., Armaly, B.F., 2004. Reverse flow regions in three-dimensional backward-facing step flow. *Int. J. Heat Mass Tran.* 47, 4713-4720.
- Schrott, W., Svoboda, M., Slouka, Z., Snita, D., 2009. Metal electrodes in plastic microfluidic systems. *Microelectron. Eng.* 86, 1340-1342.
- Sherry, M., Lo Jacono, D., Sheridan, J., 2010. An experimental investigation of the recirculation zone formed downstream of a forward facing step. *J. Wind Eng. Ind. Aerodyn.* 98, 888-894.
- Stogiannis, I.A., Mouza, A.A., Paras, S.V., 2013. Study of a micro-structured PHE for the thermal management of a fuel cell. *Appl. Therm. Eng.* 59, 717-724.
- Tihon, J., Legrand, J., Legentilhomme, P., 2001. Near-wall investigation of backward-facing step flows. *Exp. Fluids* 31, 484-493.
- Tihon, J., Pěnkavová, V., Pantzali, M., 2010. The effect of inlet pulsations on the backward-facing step flow. *Eur. J. Mech. B-Fluid* 29, 224-235.
- Tylli, N., Kaiktsis, L., Ineichen, B., 2002. Sidewall effects in flow over a backward-facing step: Experiments and numerical simulations. *Phys. Fluids* 14, 3835-3845.